Inferring genetic variant causal networks by leveraging pleiotropy

Martin Tournaire[1], Asma Nouira[1], Mario Favre Moiron[1], Yves Rozenholc[1], Marie Verbanck[1,2]

[1] *UR 7537 BioSTM, Biostatistique, Traitement et Modélisation des données biologiques, Université Paris Cité.* [2] *Inserm U900, Institut Curie, PSL Research University, 75248 Paris, France.*

Abstract

Genetic variants have been associated with multiple traits through genome-wide association studies (GWASs), but pinpointing causal variants and their mechanisms remains challenging. Molecular phenotypes, such as eQTLs, are routinely used to interpret GWAS results. However, much concern has recently been raised about their weak overlap. Taking the opposite approach with PRISM (Pleiotropic Relationships to Infer the SNP Model), we leverage pleiotropy to pinpoint direct effects and build variant causal networks. PRISM clusters variant-trait effects into trait-mediated, confounder-mediated, and direct effects, and builds individual variant causal networks by cross-referencing results from all traits. In simulations, PRISM demonstrated high precision in identifying direct effects and reconstructing causal networks. Applying PRISM to 61 traits and diseases from UK Biobank, we found that direct effects accounted for less than 13% of significant effects, yet were highly enriched in heritability. Multiple lines of evidence showed that PRISM causal networks are consistent with established biological mechanisms.

Introduction

Over the past 20 years, Genome Wide Association Studies (GWASs) have established a myriad of associations between genetic variants and human traits[1,2]. A GWAS measures and statistically tests the association between several million genetic variants and one trait of interest. According to the GWAS catalog inventory[3], 6,960 publications and 668,514 unique genetic variant-trait associations have been reported as of August 2024. However, GWASs suffer from multiple limitations and biases. First, a major issue is pleiotropy, *i.e.* a single genetic element affecting more than one trait, known to be pervasive throughout the human genome[4–6]. Because of pleiotropy, genetic variants are often associated with multiple traits in GWASs[7]. Second, it has been shown that most identified genetic variants are intergenic and involved in the regulation of the expression[8]. Consequently, the link between genetic variants and genes, and the underlying biological mechanisms, remain largely unresolved. A systematic review from 2022 reported only 309 experimentally validated non-coding GWAS variants[9]. Third, Linkage Disequilibrium (LD), referring to the non-random association of alleles at different loci on a chromosome, make GWAS results challenging to interpret since LD makes candidate causal variants in a genomic locus indistinguishable[10]. Therefore, precisely pinpointing true causal genetic variants to the complex traits they affect proves to be a tremendous challenge[11], hence the need for computational approaches complementary to GWASs.

The most prominent method to pinpoint causal variants is fine-mapping which aims at distinguishing between causal genetic variants and non-causal variants, using LD reference panels and genomic annotations[11]. Simply put, the objective is to attribute the real effect to a minimal subset of top variants in LD within a locus (at best, 1), and disqualify the other variants as LD effects. However, fine-mapping heavily relies on annotations to discriminate between causal and LD effects[12–14]. And yet recently, much concern has been raised about the fact that genetic variants overlap very little with annotations like molecular quantitative trait loci (QTL), particularly expression QTL (eQTL)[15,16]. To the point that GWAS and cis-eQTL variants show systematic structural differences[17]. Likewise, GWAS and EWAS (epigenome-wide association studies) do not find the same causal genes[18].

Here, we take the opposite view to traditional fine-mapping methods, to completely sever our approach from annotations. Instead, the idea is to take advantage of the omnipresence of pleiotropy to disentangle variant-trait associations obtained from GWAS. Apart from LD, we hypothesize that these associations can be explained by 3 distinct underlying biological mechanisms: 1) direct effect when the association is caused by a true causal direct effect from variant to trait; 2) vertical pleiotropy when the association can be explained by a variant-trait effect on another trait, which in turn affects the primary trait; 3) confounder pleiotropy when the association can be explained by a confounder between traits. Therefore, to disentangle the variant-trait associations, we propose to leverage pleiotropic relationships between traits by rerouting an integrative Mendelian randomization (MR) method.

MR aims to infer the causality of an exposure trait X on an outcome trait Y. MR uses genetic variants as instrumental variables that are robustly associated with the exposure of interest and tests whether the effects of the variants on the exposure result in proportional effects on the outcome. Classical MR relies on three assumptions: 1) the genetic variants must be strongly associated with the exposure X; 2) the genetic variants cannot directly affect the outcome Y; 3) the genetic variants must not affect the confounder U of the exposure-outcome relationship. It has been shown that traditional MR massively suffers from pleiotropy, which violates the assumptions and biases the results[19]. This led to the development of multiple integrative MR methods that takes into account pleiotropy, notably by modelling a latent confounder (*e.g.* LHC-MR[20], CAUSE[21], MR-CUE[22]). However, MR only uses genetic variants as instrumental variables, and no conclusions are drawn on individual variant-trait associations. Therefore, we chose to reroute MR to focus on the relationships between variants and traits.

Here, we propose PRISM, which stands for Pleiotropic Relationships to Infer the SNP model, a genome-wide method to disentangle variant-trait associations from GWASs, into vertical, confounder, or direct effects. The rationale behind PRISM is to re-examine variant-trait associations from GWAS through the prism of all other traits. Concretely, PRISM runs a pairwise MR model that integrates a confounder, across all studied traits. Then, by aggregating results from all pairwise iterations, PRISM predicts significant variant-trait effects, that are consistent regardless of the pleiotropic trait context. Finally, PRISM reconstructs the causal network for each variant, assigning labels to all significant variant-trait effects. To assess the performances of PRISM, we simulated GWAS summary statistics for a complex network of traits. Then we processed 61 heritable traits from UK Biobank[23] through PRISM and disentangled the effects of ~4 million variants to infer causal networks.

Results

PRISM disentangles the associations of genetic variants from GWASs by leveraging pleiotropy.

PRISM inputs GWAS summary statistics for multiple traits to infer a causal network for each genetic variant (Fig. 1). Each significant variant-trait effect is predicted and labeled as a direct or pleiotropic effect. We hypothesize that the observed associations in GWAS can be attributed to 3 distinct underlying biological mechanisms: 1) confounder pleiotropy occurs when the variant has an effect on the confounder of the relationship between traits; 2) vertical pleiotropy arises from the variant-trait effect caused by another trait; 3) a direct effect occurs when the association is due to a true causal direct effect from the variant on the trait. Therefore, variant-trait associations in GWASs are induced by true causal direct effects and their pleiotropic ripple effects. To comprehensively disentangle these associations, PRISM analyzes each single variant-trait effect across multiple contexts. Specifically, PRISM evaluates the effect of a genetic variant on a trait X relative to all other traits. It systematically assesses the variant effect on X relative to trait A, then to trait B, and so forth. By aggregating information through the prism of all other traits, PRISM identifies and predicts whether the variant-trait effect is consistent between the different contexts, and subsequently labels the effect as direct or pleiotropic. Concretely, the "confounder pleiotropy" label indicates that the variant was identified as having an effect on trait X only through a confounder shared with another trait. In contrast, the "vertical pleiotropy" label denotes that the variant effect on trait X is only mediated through another trait causally related to X. Conversely, a "direct effect" means that the variant is not flagged for pleiotropy, indicating that its effect on X is not mediated by any other factor. Once this procedure is completed for all traits, the obtained direct and pleiotropic labels are used to construct a causal network for each variant and the traits it impacts.

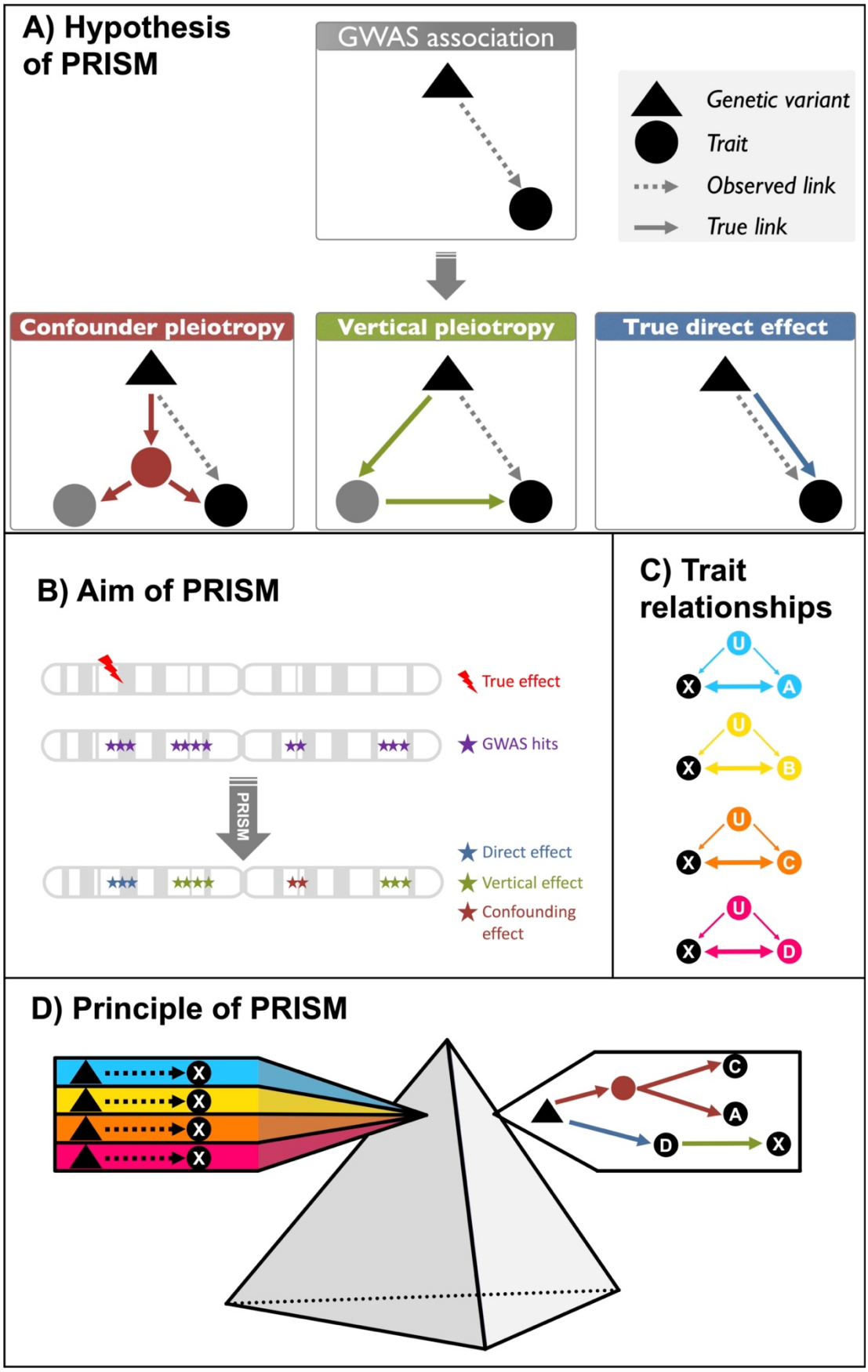

Figure 1: Overview of PRISM | ***A)*** *3 distinct mechanisms underlying GWAS associations: 1) confounder pleiotropy, i.e. effect mediated by a confounder; 2) vertical pleiotropy, i.e. effect mediated by a causal relationship between two traits; 3) direct effect.* ***B)*** *PRISM aims at disentangling GWAS associations into direct effects, hypothesized to convey true causal effects, from pleiotropic effects (vertical and confounder).* ***C)*** *Each variant-trait association is evaluated in a model of trait X in different contexts relative to trait A, then to trait B, and so on. Each model takes into account a unique latent confounder U (Supplementary Fig. 1).* ***D)*** *PRISM assesses the effects of all studied genetic variants on a trait X, through the prism of multiple trait contexts. Then, by cross-referencing the information and combining all traits, a full causal network can be built for each variant.*

PRISM accurately distinguishes direct from pleiotropic effects in simulations.

We constructed a complex pleiotropic network consisting of 18 simulated traits and 100,000 variants to generate GWAS summary statistics (See Fig. 6 and Online Methods). In a nutshell, the simulated network consisted of different groups of traits A, B, C, D and E. A connected directly to $B3$ and $B4$, and $B1$ and $B2$ had mutual causal influences while D was causal to A. $B4$ also connected to traits from the C group, which made $B4$ the most pivotal trait in our network. Traits from group E had no causal relationships with any other traits. Finally, all traits shared a unique confounder with every other trait. This structure emphasized the complex interplay of direct, vertical, and confounder relationships among traits. In addition, this network encompassed a wide array of scenarios consisting in modulating the polygenicity and the heritability of traits, the strength of causal effects between traits, and the strength of the confounders (Supplementary Table 1). Then, we processed the simulated data through PRISM, and compared the true variant-trait effects with those predicted by PRISM. We calculated the precision and recall to assess the performance of predicting each type of pleiotropy. As shown in Fig. 2 and Supplementary Fig. 2, PRISM achieved very high precision and recall in scenarios characterized by highly heritable traits with low polygenicity and low pervasive confounder effects, regardless of causal relationships between traits. Importantly, we chose to prioritize precision over recall, even in scenarios featuring high polygenicity and high targeted confounder effects. Therefore, for highly polygenic traits and pervasive confounders, PRISM detected only a subset of all true variant-trait effects but stringently controlled for false positives.

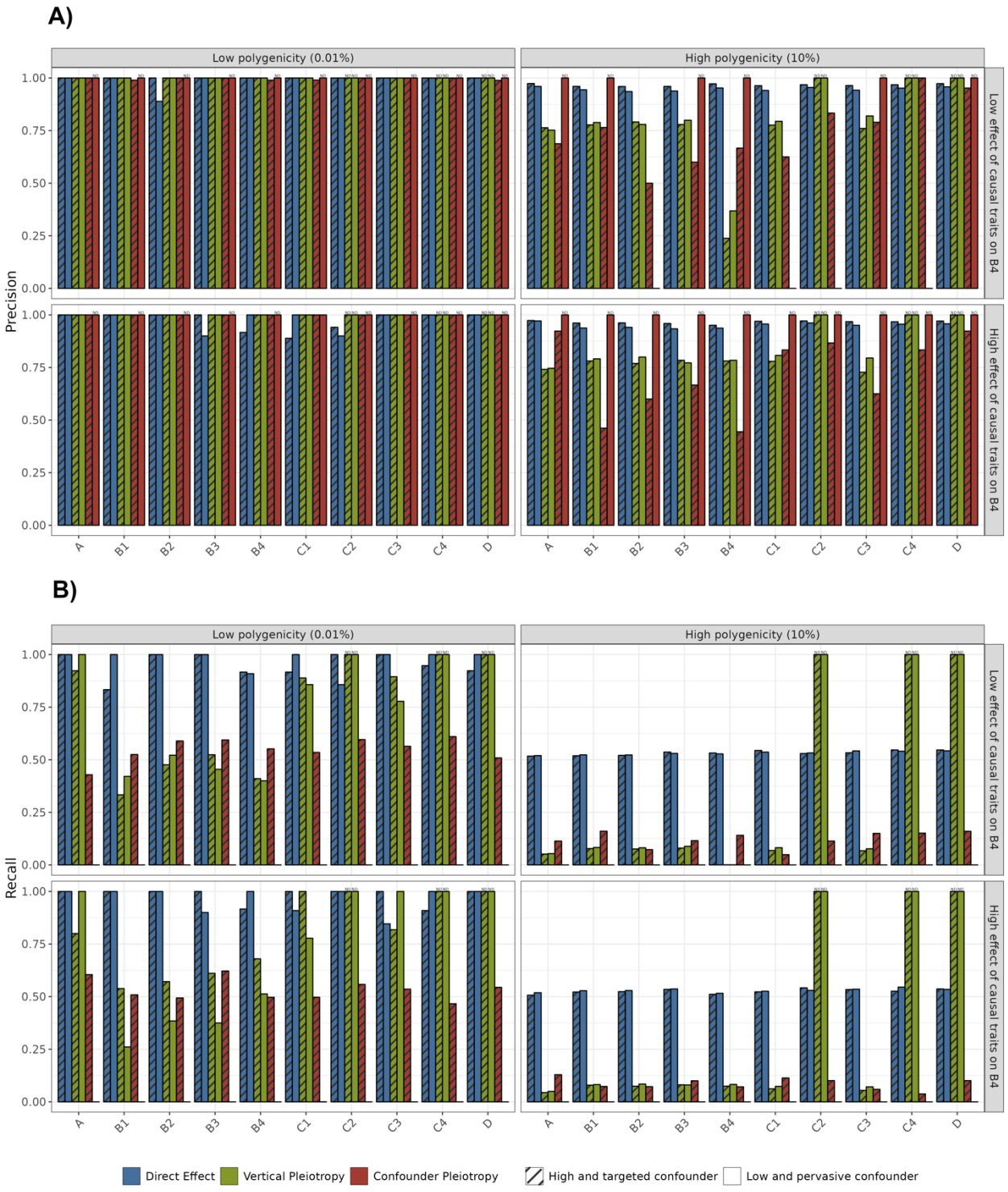

Figure 2: ***A)*** *Precision and* ***B)*** *Recall of PRISM predictions for significant variant-trait effects, on simulations. The x-axis represents the simulated traits in the network (See Fig. 6 and Online Methods). Significant effects are defined with* $P < 5 \times 10^{-8}/17$ *, the recommended threshold from PRISM (See Online Methods). Bars are colored according to predicted direct and pleiotropic labels. By convention, when variants neither exist nor were predicted for a given label, the accuracy or the recall equals 1, such cases are indicated with ND. Eight scenarios are represented across facets, with varying parameters. Polygenicity represents the proportion of variants with a direct effect on each trait. Effect on* $B4$*, the most pivotal trait, represents the proportion of effect passed to* $B4$*, for all traits with a non-zero vertical effect on* $B4$*. High targeted confounder means that few variants (0.01%) have an effect on the confounder U, but with magnitude of effect rivaling direct effects. Low pervasive confounder means that a large proportion (5%) of variants have an effect on the*

confounder, but with low magnitude. ***A)*** *The y-axis represents the precision which is the proportion of well-predicted variants among all predicted variants for a given label.* ***B)*** *The y-axis represents the recall, which is the proportion of well-predicted variants among all true variants for a given label. NB: results for traits* $E1$-$E8$ *can be found in Supplementary Fig. 2*

PRISM accurately reconstructs variant causal networks in simulations.

The end goal of PRISM is to use predicted and labeled variant-trait effects to construct a causal network for each variant. A network consists of nodes that represent the variant and the traits it significantly affects, and edges that represent the variant-trait and trait-trait effects labeled as direct or pleiotropic. In our simulations, we applied a weighted Simple Matching Coefficient (SMC) to individually compare the variant networks predicted by PRISM with their true simulated counterparts. First, we measured the accuracy of the predicted networks by matching their edges with those of the true networks. As illustrated in Supplementary Fig. 3, the predicted edges from PRISM are either identical or very similar to those of the true networks. Second, we measured the power of detecting true networks by matching their edges with those of the predicted networks. As shown in Supplementary Fig. 4, PRISM-predicted networks are often incomplete, especially in scenarios with high polygenicity, as the method lacks sufficient power to detect all variant-trait effects. However, this is a deliberate methodological choice to stringently control for false positives. In other words, although the networks built by PRISM might be incomplete, the inferred edges are very likely to represent true effects.

PRISM complements traditional fine-mapping methods.

PRISM adopts a fundamentally different approach compared to traditional fine-mapping. Instead of distinguishing between variants in LD, PRISM predicts whether variant-trait effects are direct or caused by pleiotropy. Still, we evaluated the compatibility of PRISM with standard fine-mapping methods, such as SuSiE[24,25], CARMA[13], and FINEMAP[26]. Since fine-mapping must be conducted on a single trait, we chose to focus on the most pivotal trait in our simulated network ($B4$, Fig. 6) in a highly heritable and polygenic scenario (scenario 24, Supplementary Table 1) and focused on true causal variants. Firstly, we assessed PRISM precision in identifying true causal variants as direct effects. Then we compared it to the precision of the fine-mapping methods in prioritizing true causal variants within the fine-mapped set. In this scenario, PRISM achieved a precision of 95%, outperforming the fine-mapping methods which had precision rates ranging from 86% to 89%. It is worth mentioning that both PRISM and traditional fine-mapping methods were mainly misled by high targeted confounder variant-trait effects. However, PRISM exhibited a recall of 51%, significantly higher than the below 1% recall observed for the fine-mapping methods. Indeed, fine-mapping methods are designed to identify a limited number of variants within a locus, whereas PRISM operates on a genome-wide scale. These findings indicate that for highly polygenic traits, PRISM is more efficient in identifying causal variants at the genome scale compared to fine-mapping methods that focus on specific loci.

PRISM reassesses GWAS variant-trait associations and distinguishes between direct and pleiotropic effects.

PRISM tests and labels variants for direct and pleiotropic (*i.e.* vertical and confounder) effects on a panel of traits. Contrary to GWAS, an effect is considered as PRISM significant if it remains consistent across multiple assessments in different contexts. We

processed 61 heritable traits with GWAS summary statistics from UK Biobank[23] through PRISM (Supplementary Table 2) and compared p-values from GWAS and PRISM. To illustrate how PRISM processed GWAS associations, let us take the concrete and representative example of coronary heart disease (CHD) (Supplementary Fig. 5). First, the majority of the 947 significant variants were classified as having vertical or confounder effects by PRISM, with 441 and 497 variants respectively. Only 6 variants were identified as having direct effects, all mapping to the non-coding gene CDKN2B-AS1. A recent study[27] highlighted its potential role in CHD by acting as an RNA-sponge regulating microRNA miR-92a-3p, a known therapeutic target of CHD[28–30]. This explains why PRISM did not trace the effect to any other trait in the framework. Second, the vast majority of highly significant GWAS variants were labeled with confounder effects. Third, closely examining the causal networks of pleiotropic (vertical and confounder) variants revealed that most variant effects on CHD are mediated by lipids. In summary, PRISM tests and evaluates genetic variant effects, offering deeper insights into the biological mechanisms underlying associations observed in GWAS.

PRISM reveals that most observed associations in GWAS summary statistics are caused by relationships between traits.

Generalizing to all variant-trait effects, we observed that direct effects represent less than 13% of all PRISM significant effects, while confounder and vertical pleiotropy represent 44% and 43% respectively. Since PRISM leverages pleiotropy, we aimed to characterize the pleiotropic nature of the associations discovered in GWASs. Indeed, GWASs often reveal numerous observed pleiotropic associations, where a genetic variant demonstrates significant associations with at least two traits. Specifically, we identified 170,433 variants exhibiting observed pleiotropic effects from GWASs. Therefore, we assessed the nature of this pleiotropy using PRISM. Naturally, confounder and vertical effects provide us with straightforward pleiotropic effects. However for direct effects, we defined the horizontal pleiotropic effect (also denoted true pleiotropy or uncorrelated pleiotropy) when a genetic variant has a direct effect on two traits. Using PRISM on the 61 highly heritable traits, we found that confounder and vertical pleiotropies were responsible for respectively 66.8% and 33% of the observed pleiotropy in GWAS across all traits (Fig. 3 and Supplementary Fig. 6). Thus, horizontal pleiotropy, true multiple direct causal effects from a genetic variant, was found extremely rare and represented 0.2%. This finding underscores the complexity of genetic effects on multiple traits and highlights the effectiveness of PRISM in elucidating the underlying mechanisms of pleiotropic associations in GWAS findings.

Figure 3: Heatmap of variant effects shared between traits. The bottom-right triangle represents the proportion of GWAS significant variants shared between traits. The grey tile gradient represents the observed pleiotropy from GWAS (scaled proportions). The top-left triangle represents the largest proportion of PRISM significant variants classified in one of the three categories of pleiotropy between the pair of traits (confounder, vertical, or horizontal). The red, green and blue tile gradients represent confounder, vertical and horizontal pleiotropy respectively (scaled proportions). The diagonal represents the proportion of individual direct effects for each trait.

PRISM Direct variants are significantly enriched in per-variant heritability compared to GWAS variants and pleiotropic variants.

In GWAS, variant heritability measures the proportion of the trait variance explained by all measured variant associations. Thus, the per-variant heritability is the contribution of a specific genetic variant to the overall heritability. We applied stratified LD score regression[31] (s-LDSC) to calculate per-variant heritability enrichments across labeled variant-trait effects grouped into four categories: three categories for PRISM significant variant effects (direct, vertical, confounder), and a category for GWAS significant associations. Across most traits, we observed a consistent order in the enrichment (Fig.

4). Indeed, direct variants demonstrated higher enrichment in per-variant heritability compared to GWAS variants, which in turn exhibited higher enrichment than vertical variants, followed by confounder variants. This highlights the hypothesis that indirect pleiotropic effects on traits are weaker compared to direct effects.

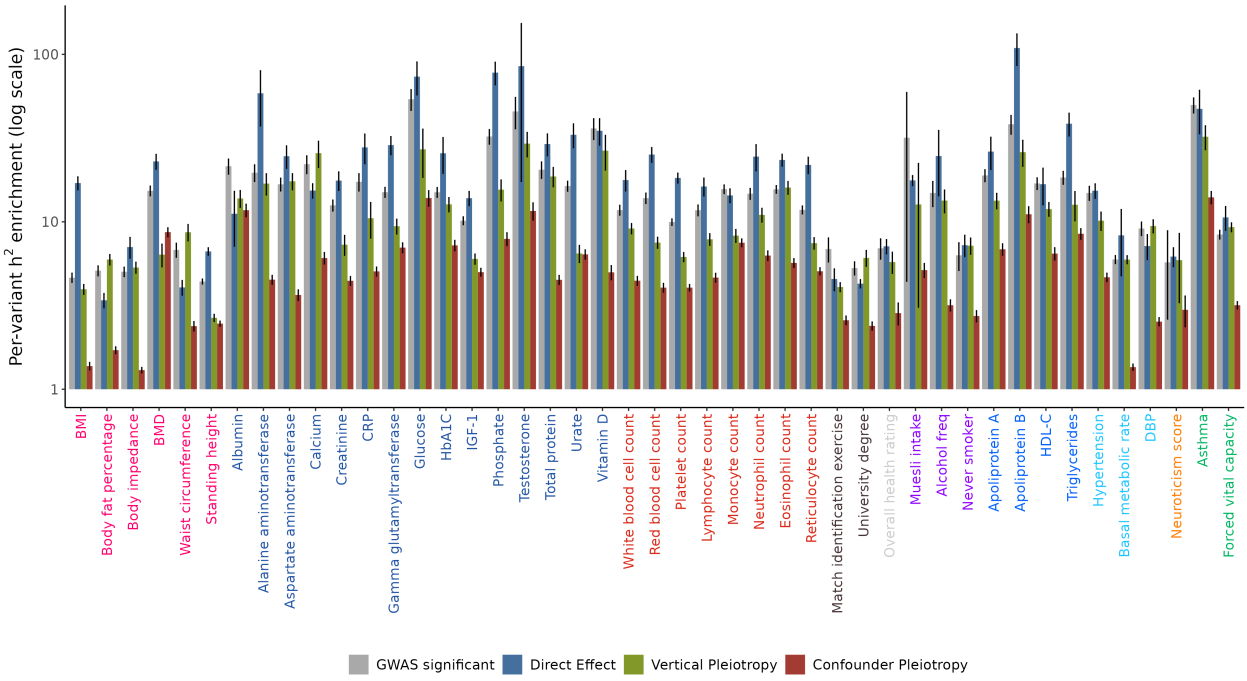

Figure 4: Enrichment in per-variant heritability of genetic variants, according to PRISM categories (direct, vertical, confounder) and GWAS. The x-axis represents the traits colored by broad categories. The y-axis represents enrichment in per-variant heritability, calculated with stratified LD score regression. The enrichment is represented in a log scale.

PRISM produces coherent results on a panel of literature-validated variants.

The final aim of PRISM is to infer causal networks for genetic variants. To confirm the reliability of PRISM, we aimed to compare its predicted networks to what the scientific literature suggests. For some networks of interest, we therefore examined whether the variant-trait effects identified and labeled by PRISM had already been previously identified. For example, variant rs7528419, residing in the SORT1 gene locus[32] coding for the sortilin protein, were strongly associated with coronary heart disease (CHD) in GWAS[32]. According to PRISM (Fig. 5A), this variant displayed a vertical effect on CHD but a direct effect on apolipoprotein B (apoB). Essentially, PRISM suggested that this variant affects CHD only through its direct effect on apoB, which has a causal effect on CHD. Recent studies have indeed demonstrated that sortilin restricts the secretion of apoB[33], and that apoB is one of the most accurate markers of lipid-induced cardiovascular risk[34]. Another example of validated network is rs2282679, mapped to gene GC[35], which is validated for vitamin D levels. Kew et al.[36] also highlighted that this gene is involved in white blood cells and neutrophil accumulation. Remarkably, these findings align with the 3 direct effects identified by PRISM coming from these variants (Fig. 5B). Additional validated networks can be found in the Supplementary Results.

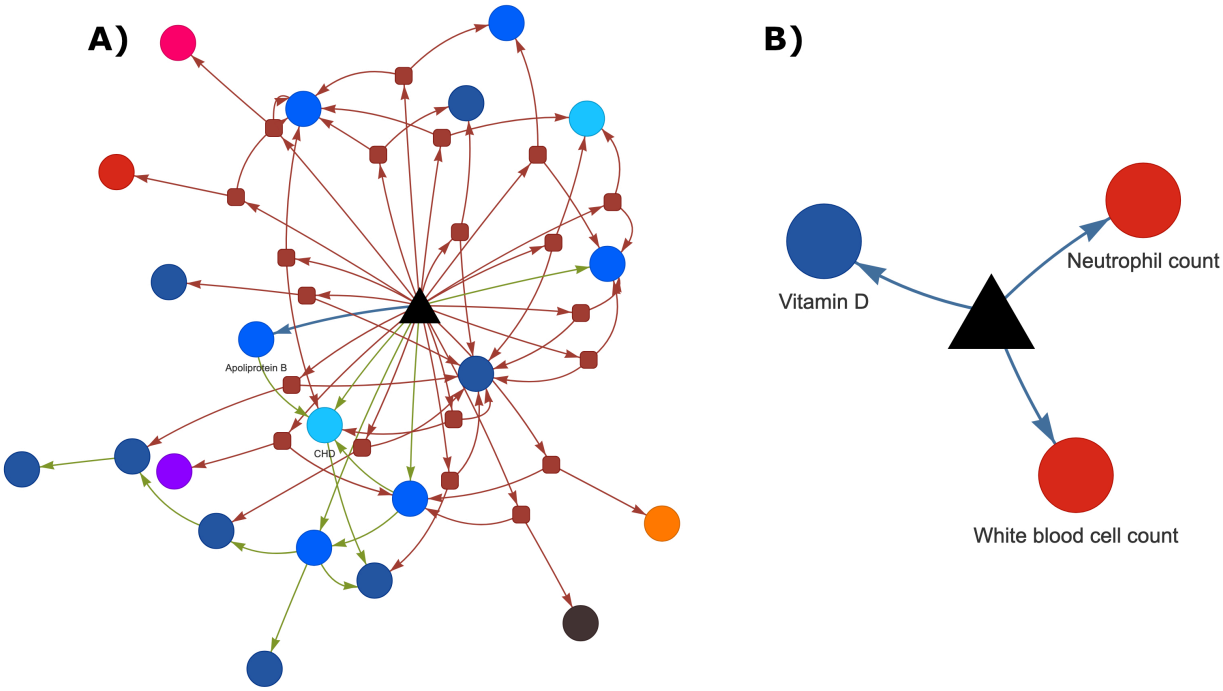

Figure 5: PRISM inferred causal network for variants rs7528419 (A) and rs2282679 (B). Genetic variants are represented as black triangles. Red arrows are effects of the variant through a confounder meaning confounder pleiotropy. Green arrows are effects of variant through a causal trait meaning vertical pleiotropy. Blue arrows are direct causal effects from the variant to traits. Confounders are represented as red squares and traits are represented as circles colored according to trait categories.

PRISM variants mapped to eGenes are found in relevant tissues.

Standard follow-up analysis in GWAS involves checking whether the associated variants are eQTL in tissues linked to the studied trait. We expect to identify more interpretable and relevant eGenes using PRISM direct and pleiotropic categories. A concrete example of interpretability is provided for coronary heart disease (CHD), where we investigated the enrichment of relevant tissues in the expression of genes associated with eQTL variants identified by PRISM. We retrieved eQTLs and their corresponding eGenes through GTEx[37] (Supplementary Fig. 7). Overall, enrichments were more pronounced for PRISM than GWAS, and we observed 3 enrichment peaks above 2 for PRISM and none for GWAS, each providing valuable insights. The liver was enriched in vertical pleiotropy, suggesting a lipid-mediated effect from the liver. The brain anterior cortex was enriched in confounder pleiotropy, which hinted at CHD comorbidity with obesity, hence linked to brain functions. Similarly, lymphocyte cells were enriched in confounder pleiotropy, which hinted at a potential association between CHD, obesity and chronic inflammation. These examples showed that PRISM direct and pleiotropic categories reflect specific underlying biological mechanisms.

PRISM pinpoints direct variants that are mapped to more trait-specific genes than GWAS.

Traditional pipelines for GWAS analysis typically involve examining genes mapped to significant variants, and their associated pathways. In our study, we notably performed annotation analysis to map functionally annotated variants to genes based on their physical positions in the genome and expression Quantitative Trait Locus (eQTL)

mapping. To provide a comprehensive view across all traits, we utilized FUMA[38], a powerful tool for conducting extensive functional annotation analyses. Supplementary Fig. 8 illustrates the strong connectivity of traits through GWAS mapped genes. Upon examining genes mapped to PRISM direct variants, we observed a much smaller number of common genes among traits. Supplementary Fig. 9 illustrates that most genes shared between traits were involved in vertical or confounding pleiotropy. These observations suggest that genes mapped to direct variants may be more relevant, resulting in a simpler and more biologically interpretable variant-gene-trait network from PRISM. To further investigate the biological significance of our results, we conducted an enrichment analysis based on DisGeNET[39] pathways using genes mapped to PRISM direct and GWAS variants. The goal was to identify enriched pathways and compare their significance between PRISM direct- and GWAS-mapped pathways. As shown in Supplementary Fig. 10, PRISM direct pathways exhibited significantly greater enrichment compared to GWAS pathways in more than two-thirds of the traits with significant differences. Next, we employed bipartite network analysis to compare the centrality measures of gene-trait networks constructed from PRISM direct and GWAS variants. In Supplementary Fig. 11, PRISM network demonstrated lower degree and closeness, indicating fewer links between traits, but higher betweenness, suggesting the presence of more central traits. To ensure a fair comparison despite the fewer PRISM direct genes compared to GWAS genes, we conducted two distinct methodologies. First, we randomly removed genes from the GWAS network while retaining the edges linked to the selected genes. This resulted in centrality measures similar to those of the full GWAS network (black dots). Second, we removed both genes and edges to create GWAS sub-networks with the same number of nodes and edges as the PRISM direct network. Remarkably, with networks of the same dimension as PRISM, the centrality measures were equivalent for all the traits (red dots), and PRISM network still demonstrated lower degree and closeness. This suggests that the network inferred from PRISM direct variants was denoised and untangled, discarding redundant and biased relations induced by pleiotropy.

Discussion

We developed PRISM (Pleiotropic Relationships to Infer the SNP model) that aims at reassessing the associations between genetic variants and traits from GWAS, by distinguishing between direct effects and pleiotropic effects. *In fine*, PRISM infers a causal network for each genetic variant. PRISM takes the opposite view to current methods such as fine-mapping, and does not resort to any annotation but instead leverages pleiotropy which is pervasive throughout the human genome. We assessed the performances of PRISM on a simulated complex pleiotropic network of traits and compared it with several other fine-mapping methods. We fine-tuned PRISM to achieve high precision in predicting direct and pleiotropic variant-trait effects, which resulted in limited power to detect significant variant-trait effects in highly polygenic traits. Consequently, causal variant networks predicted by PRISM, although often incomplete, demonstrated a high level of accuracy. We applied PRISM to a set of 61 heritable traits and diseases from UK Biobank. PRISM was able to build a causal network for 371,551 unique variants. PRISM showed that most GWAS associations were caused by pleiotropy, as only 13% of variant-trait effects were direct. Direct variants predicted by PRISM were significantly enriched in per-variant heritability compared to GWAS significant variants and pleiotropic variants. Comparing biological pathways derived from PRISM direct variants and GWAS variants,

the enrichment was stronger for PRISM. PRISM was able to pinpoint direct variants mapped to more trait-specific genes than GWAS, and the PRISM gene-trait network appeared disentangled and more pertinent compared to the GWAS gene-trait network. PRISM inferred relevant variant causal networks; we could show the concordance between the causal networks inferred by PRISM and the networks from the literature for a panel of validated variants. Importantly, each causal network constructed by PRISM is specific to its corresponding variant. All significant edges in these networks are computed by PRISM, which is different from integrating variants into pre-existing trait networks.

However, the proposed method has a number of limitations. First, PRISM is highly dependent on the set of processed traits. Indeed, pleiotropy is relative to the traits in the network, and so are the direct and pleiotropic labels. Depending on the shape of the network, some effects can be justifiably classified as vertical or confounder pleiotropy. Adding or removing traits, especially central traits, can have an impact on whether or not the variants are significant, and their type of pleiotropy (See Supplementary Results for details). Second, PRISM heavily relies on parameters computed by LHC-MR to assess the relationships between traits and to infer direct and pleiotropic labels. We tested PRISM performances with noisy parameters, and concluded that PRISM precision and recall are robust to reasonable parameter estimation errors (See Supplementary Results for details). Third, PRISM is geared towards precision to identify direct variant-trait effects. Hence confounder and vertical precision are more limited, as is the overall power of PRISM. This is a deliberate choice since we aim to favor precision in the identification of direct effects. Fourth, the precision and recall were calculated from summary statistics simulated from a pleiotropic network of heritable traits. Similarly on real data, we only included heritable traits. Traits that are not heritable might disrupt the inferred causal network. Interpreting results that include low heritability traits, which will be mechanically disadvantaged in comparison with highly heritable traits, must be performed with caution. However, we did simulate networks without any pleiotropy, and PRISM was still able to identify direct effects correctly (See Supplementary Results for details). Traits with very simple genetic architecture (*e.g.* monogenic diseases) can seemingly be processed without any issue. Fifth, as far as computational time is concerned, PRISM is limited by the pairwise step, where every possible pair of traits must be analyzed by LHC-MR. The number of such pairwise computations increases exponentially as the number of traits increases.

PRISM takes an orthogonal approach to traditional fine-mapping methods, and aims not to distinguish between variants in linkage disequilibrium (LD), but to assess whether the observed effect of a variant on a trait can be explained by pleiotropy, *i.e.* by another trait or a confounder. This has two main implications. First, we did not clump genetic variants when presenting biological results, to avoid eliminating the true causal variant effect in favor of an LD effect. Nevertheless, LD is taken into consideration when calculating the probabilities of genetic variants to have causal effects. Variants with high LD scores are penalized because they are expected to mechanically exhibit larger effect sizes[40]. Second, comparing PRISM with other fine-mapping methods is debatable since they differ in aim and approach. Fine-mapping methods primarily focus on functional genetics and, apart from LD, do not challenge the underlying biological mechanisms of associations, whereas PRISM leverages these mechanisms. Despite these differences, we undertook the comparison for two key reasons: to demonstrate that PRISM has comparable precision in identifying causal variant-trait effects, and to highlight the compatibility of

these orthogonal approaches. Fine-mapping methods, such as SuSiE[24,25], can complement PRISM by deciding between multiple candidate direct causal variants in LD. Combining these methods could enhance the identification of true causal variants within a locus and provide insights into the pleiotropy of the variants, which is crucial for future research on putative causal variants.

On a different note, direct effects and vertical pleiotropy are straightforward concepts, while confounder pleiotropy presents a greater complexity. When a variant-trait effect is attributed to confounder pleiotropy, it indicates that the effect is mediated by an unidentified factor that PRISM could not precisely determine. This factor might be missing from the analysis, or the signal could be too entangled or underpowered to distinctly identify its origin. We hypothesize that, biologically, all instances of confounder pleiotropy could actually be vertical pleiotropy, where the mediating factor has yet to be clearly identified.

PRISM underlying model implies that direct effects result in stronger effect sizes in GWAS summary statistics. It would be a legitimate question to ask if direct variants are simply the most significant variants with the strongest effect sizes, while confounder and vertical variants are weaker significant variants. But although direct variants tend to have higher initial Z-scores from GWAS, PRISM results show much more intertwined results when looking at the original Z-scores of the different pleiotropies (Supplementary Fig. 12). For simple molecular traits like lipids or biomarkers, direct variants do tend to have higher Z-scores. However, complex traits like respiratory or metabolic traits do not follow this trend. In conclusion, we are confident that PRISM can effectively distinguish between subtle biological mechanisms.

We concluded that the gene network inferred from PRISM direct variants is denoised and disentangled compared to the network inferred from GWAS variants. This observation raises the question of whether the reduced complexity of the PRISM-inferred network is due to PRISM limited power, potentially resulting in the detection of fewer significant variant effects and, consequently, a simpler network. However, our analysis suggests otherwise. We demonstrated that, even when reduced to the same number of nodes and edges as the PRISM network, the GWAS network still exhibited the tangled characteristics of the full GWAS network.

To develop the method, we prioritized statistical power by selecting a cohort with a large sample size, specifically the UK Biobank, and could suffer from issues related to sample overlap. However, the bias from sample overlap is expected to be small when using a large sample size[20,41]. Another consequence of using UK Biobank, is that all the GWAS associations were obtained on individuals from “white British” ancestry[23]. Therefore, it would be valuable to apply PRISM to other ancestries and compare the inferred variant networks across different populations. Additionally, these results only cover common variants, as associations with rare variants are underpowered in GWAS[42]. Finally, these results are restricted to HapMap3 variants, but PRISM could be extended to more common variants.

Horizontal pleiotropy, defined as true multiple direct causal effects from a single genetic variant, is surprisingly rare, accounting for only 0.2% of the observed pleiotropy in GWAS. In simulations, PRISM reliably detected horizontal variant-trait effects across a wide range of scenarios (See Supplementary Results for details). Therefore, we strongly believe that

genetic variants with completely independent effects on multiple traits are extremely rare in the human genome, as we have previously shown[7].

To conclude, at the trait level, PRISM can be used to better apprehend the genetic architecture of complex traits and the relationships between traits. At the variant level, PRISM can help understanding the specific genetic effect of a variant on multiple traits. We strongly believe that building the causal network of genetic variants is a priority to guide in vitro and in vivo follow-up studies as well as for medical applications, like genomic medicine or genome editing.

Online Methods

General principle of the PRISM - Pleiotropic Relationships to Infer the SNP Model - method.

General aim: PRISM infers causal networks for genetic variants.

The general objective of PRISM is to infer causal networks for genetic variants from GWAS summary statistics, distinguishing between direct and pleiotropic effects. Essentially, PRISM evaluates variant-trait effects across multiple contexts, systematically assessing the impact of all genetic variants on a trait X in relation to other traits. By aggregating information from these contexts, PRISM identifies consistent variant-trait effects and classifies them as direct or pleiotropic. “Confounder pleiotropy” indicates a variant that affects trait X solely through a shared confounder with another trait. “Vertical pleiotropy” indicates a variant that affects trait X through another trait that causally affects X. “Direct effect” indicates that the variant affects X without any mediation by any other trait or confounder. Upon completing this analysis for all variant-trait effects, the results are combined to construct a comprehensive causal network for each variant disentangling the effect of the variant on all the traits.

Pairwise step: PRISM models variant-trait associations in a pairwise trait context.

Let X and Y denote two traits, and U a latent confounder with causal effects on both X and Y (Supplementary Fig. 1). X and Y may have direct causal effects on each other. Let $\mathbf{G}$ represent the genome-wide genotype data for m genetic variants. Let $\hat{\beta}_k^x$ and $\hat{\beta}_k^y$ denote the standardized effects of a genetic variant k on traits X and Y respectively, observed from GWAS summary statistics. We model an 8-component bivariate Gaussian Mixture Model. Each component corresponds to the expected distribution of standardized effects from variants in that particular component. The eight components are: (0) No association; (1) Associated with X; (2) Associated with U; (3) Associated with Y; (4) Associated with X and U; (5) Associated with X and Y; (6) Associated with U and Y; (7) Associated with X, Y and U.

Each variant effect is hypothesized to be drawn from one of these components. The probability that a given variant k belongs to Gaussian component j is determined by the following posterior probability:

$$\hat{P}\left(k \in j | \hat{\beta}_k^x, \hat{\beta}_k^y\right) = \frac{\phi\left(\hat{\beta}_k^x, \hat{\beta}_k^y | 0, \widehat{\mathbf{\Omega}}_\mathbf{j}\right)\hat{P}(k \in j)}{\sum_{i=0}^{7} \phi\left(\hat{\beta}_k^x, \hat{\beta}_k^y | 0, \widehat{\mathbf{\Omega}}_\mathbf{i}\right)\hat{P}(k \in j)}$$

Here, $\widehat{\mathbf{\Omega}}_{\mathbf{j}}$ denotes the variance-covariance matrix of Gaussian component j. The function ϕ represents the joint probability density function of the bivariate normal distribution, and $\hat{P}(k \in j)$ is the prior probability of variant k belonging to component j.

For each variant k, we compute the probability of belonging to each component. Then, we translate these probabilities into three scores corresponding to the variant having no effect, or an effect on X, or on Y. No Effect: the score indicating no effect of variant k on neither X nor Y corresponds to the probability of belonging to component (0). Effect on X: the score indicating an effect of variant k on X corresponds to the highest probability among the components that include an effect on X, specifically components (1), (4), (5) and (7). Effect on Y: the score indicating an effect of variant k on Y corresponds to the highest probability among components indicating an effect on Y, specifically components (3), (5), (6) and (7).

Parameter estimation: PRISM uses global trait pleiotropic relationships parameters.

To apply PRISM pairwise step to a pair of traits, we need to estimate $\widehat{\mathbf{\Omega}}_{\mathbf{j}}$ and $\hat{P}(k \in j)$. As described in the Supplementary Methods, $\widehat{\mathbf{\Omega}}_{\mathbf{j}}$ and $\hat{P}(k \in j)$ can be expressed using the number of genetic variants m, the sample size of each trait, and a set of global parameters θ that quantifies the bidirectional causal effects between X and Y, the effects of the confounder, both trait heritabilities, and both trait polygenicities, as well as their respective LD score intercepts. The estimation of θ is performed using LHC-MR[20], an integrative Mendelian Randomization method that accounts for a latent heritable confounder. LHC-MR takes as inputs the GWAS summary statistics for a pair of traits and outputs a set of θ parameters. Since LHC-MR and PRISM share a similar underlying mathematical model, the θ parameters estimated by LHC-MR can be used as input for PRISM.

Analysis pipeline: PRISM tests and classifies variant-trait associations.

Supplementary Fig. 13 provided an overview of PRISM full analysis pipeline. Consider a set of T traits processed through the PRISM pipeline. The PRISM pairwise step evaluates all $\frac{T(T-1)}{2}$ possible pairwise combinations of these traits. This step generates scores describing the effects of each variant on each trait, measured across $T-1$ pairings (each trait paired with every other trait). By aggregating these scores for each trait, we test the significance of all possible variant-trait associations and classify all significant associations in our framework.

For example, let us consider the variant-trait association of variant k on trait X. First, we aggregate all scores indicating of an effect on trait X involving k. We define μ_k^X as the average of these scores. Similarly, we aggregate all scores indicating of the absence of effect on trait X involving k. We define μ_k^O as the average of these scores. Second, we compare both average scores using a paired Student test ($H_0: \mu_k^X = \mu_k^O$ and $H_1: \mu_k^X > \mu_k^O$) to determine significant effects. Third, we apply a Bonferroni correction to identify a significant variant-trait effects, in addition to the usual GWAS threshold of $p < 5 \times 10^{-8}$. Thus, the effect of variant k on trait X is considered significant at $\text{p-value}_k^X < \frac{5\times10^{-8}}{T-1}$.

Significant variant-trait effects are classified as confounder pleiotropy, vertical pleiotropy, or direct effect, based on the previously calculated probabilities in the different Gaussian Mixture Models (See Supplementary Methods for details).

Finally, for each variant, we construct the causal network model by creating a graph where nodes represent the variant and traits, and edges represent the relationships inferred from PRISM (direct, vertical, or confounder effects). We refine the causal network for each variant by removing vertical edges between the variant and specific traits, conditioned on other traits involved in vertical relationships[43]. This process ensures that the causal pathways are accurately represented. Additionally, when a variant shows vertical effects on multiple traits through a common causal trait, we average the effect on the causal trait and eliminate redundant edges.

Simulation framework.

Simulating GWAS summary statistics data for a complex pleiotropic network of traits.

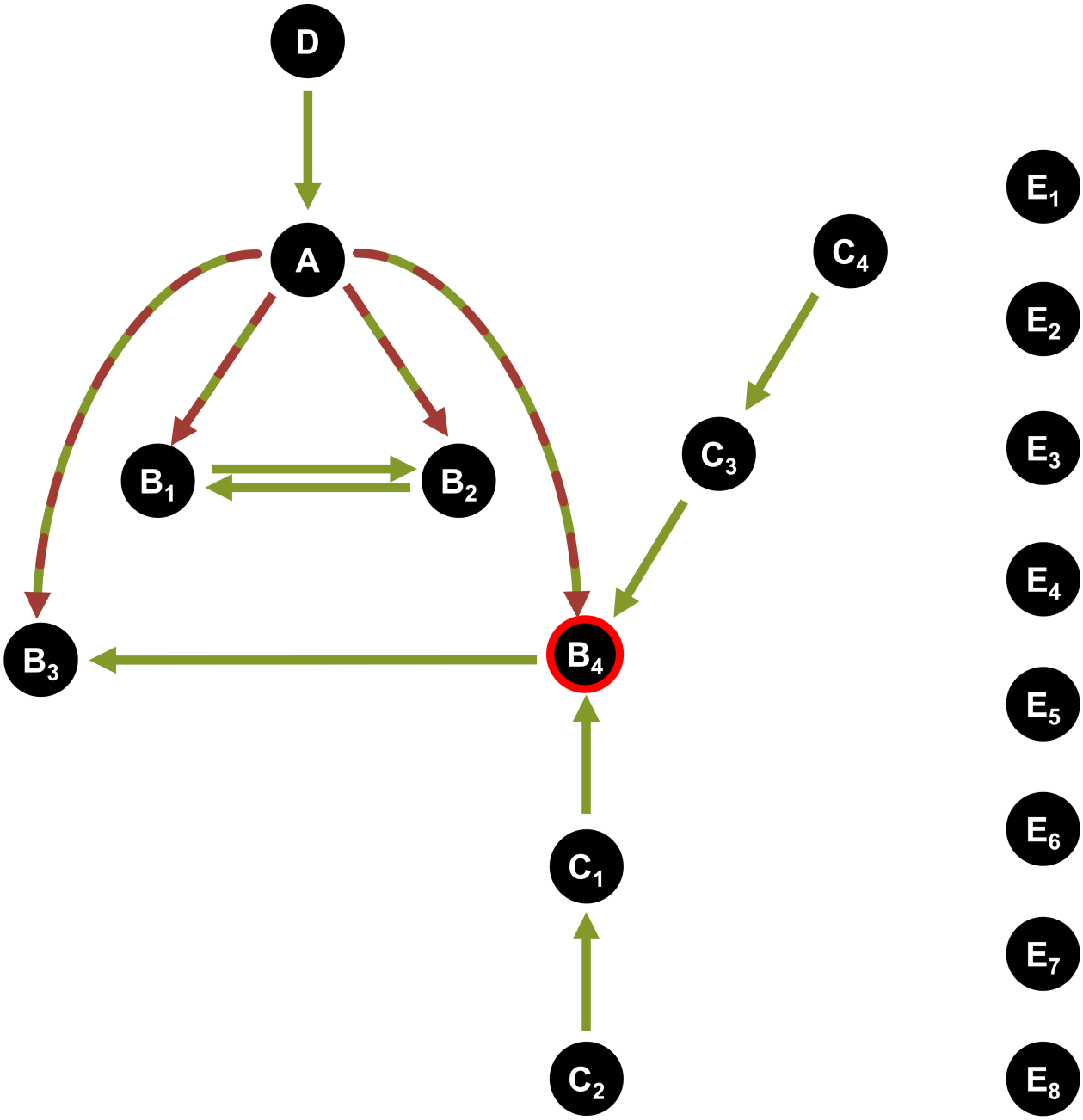

Figure 6: Architecture of the network of simulated traits. The simulated traits are represented as circles. Green arrows depict vertical relationships between traits. Striped green and red arrows depict vertical relationships between traits that can also be seen as confounder pleiotropy. For all pairs of traits, a confounder U of the relationship between a given pair of traits is added.

We started by creating an intricate network of 18 traits (Fig. 6). We created 32 different scenarios, with various parameters for heritability, polygenicity, and causal relationships, as detailed in Supplementary Table 1. To approximate a genome-wide model while maintaining computational feasibility, we opted for sets of 100,000 simulated variants. The standardized effects of all these variants on all the traits were simulated, taking into

account the relationships between the traits. First, for each trait X, we randomly selected genetic variants to have a true direct effect on trait X and on the confounders of the relationships between trait X and the other traits. For the selected genetic variants, the true direct effects were drawn from a Gaussian distribution with parameters depending on the trait and the scenario. Then, the true effects were propagated to the other traits through vertical and confounder pleiotropy. Additionally, the effects were propagated according to the LD structure of each variant. Finally, an error term was added. This produced standardized effects on all traits and LD scores for all genetic variants. The LD score of a given variant is the sum of its LD with all variants (including itself). The LD structure that we used is derived from 1000 Genomes[44] LD data from chromosome 1.

Calculating PRISM precision and recall.

For each scenario independently, we processed the simulated data through PRISM to identify and label significant variant-trait effects. The objective was to compare the true labels used during data generation against the labels inferred by PRISM. Therefore, to facilitate this comparison, the predicted label of a given LD block was determined by the label of the most significant variant. Next, the true label for each LD block was determined as follows: 1) "direct effect" if at least one variant within the block had a true direct effect; 2) "vertical effect" if at least one variant had a true vertical effect and no variants had direct effects; 3) "confounder effect" if at least one variant had a true confounder effect and no variants had direct or vertical effects; 4) "no effect" otherwise. Then, we confronted the predicted labels to the true labels by calculating the precision and recall to assess the prediction performances of each type of pleiotropy. These metrics were computed as follows for each one of the 4 labels: $\text{Precision} = \frac{\text{Number of true positive}}{\text{Number of predictions}}$ and $\text{Recall} = \frac{\text{Number of true positive}}{\text{Total number of variant-trait effects}}$.

Comparing PRISM predicted variant networks and true variant networks.

A PRISM variant network consists of nodes, representing the variant and the traits, and edges, representing the variant-trait and trait-trait effects labeled with direct and pleiotropic labels. To compare predicted variant networks with true variant networks, we regrouped edges from variants within the same LD block. Then, we applied a weighted Simple Matching Coefficient (SMC), defined as follows: $\text{SMC} = \frac{\text{Number of matching edges}}{\text{Total number of edges}}$. We implemented stringent criteria, requiring edges to be identical in terms of nodes, direction, and type of pleiotropy to be considered a match. Confounder pleiotropy inherently produces more edges than vertical pleiotropy, which in turn produces more edges than direct effects. Consequently, direct edges were assigned a weight of 1, vertical edges a weight of $\frac{1}{2}$, and confounder edges a weight of $\frac{1}{3}$.

Comparing PRISM to other fine-mapping methods.

In a scenario with high heritability, high polygenicity, and high targeted confounder effects (scenario 24, Supplementary Table 1), we evaluated the precision and recall for several fine-mapping methods CARMA[13], FINEMAP[26], and SuSiE[24,25] for trait $B4$, the most pivotal trait in our simulated network. High polygenicity combined with high confounder effects create an unfavorable and highly pleiotropic scenario, where the effects of genetic variants are complex and intertwined, with confounder effects comparable in magnitude to direct

effects. For computational reasons, Z-scores and the LD matrix were divided into 10 chunks, each containing approximately 10,000 variants independent from the others. None of the methods were provided with annotations.

Application to 61 traits from UK Biobank.

We selected 61 heritable traits and diseases with publicly available GWAS summary statistics data from UK Biobank[23] (Supplementary Table 2). Variants from the human leukocyte antigen (HLA) region on chromosome 6 were excluded due to the high density of variants associated with autoimmune and infectious diseases, and the complex LD structure in this region[20]. Variants from sex chromosomes were excluded due to the complexity of their unique inheritance patterns and gene expression differences between sexes. Low-confidence variants and rare variants with a minor allele frequency (MAF) below 0.05 were also excluded due to their insufficient statistical power. Only variants present in the HapMap3 framework were analyzed, because LHC-MR is limited to these variants. We then processed these 61 traits through PRISM.

Computing per-variant heritability enrichments.

To interpret PRISM results, we employed stratified LD score regression (s-LDSC)[31]. We calculated per-variant heritability enrichments across labeled variant-trait effects, separately for each trait. Variants were grouped into four categories: three categories (direct, vertical, confounder) for PRISM significant variant effects, and a category for GWAS significant associations. We used the same threshold for both PRISM and GWAS of p-value$^{X}_{k} < \frac{5\times10^{-8}}{60}$ corresponding to the traditional GWAS threshold divided by the number of traits -1. These categories were not mutually exclusive, as most PRISM significant variants were also GWAS significant. Only 45 traits among the 61 traits had enough variants in all four categories to be processed by s-LDSC.

eQTL and eGenes retrieval from GTEx.

We retrieved the eQTL and correspondent eGenes from GTEx[37] version 8. We converted the genomic coordinates from Hg38 to Hg19 using the liftOver R package. We identified significant variant-eGene pairs under the following threshold p-value $< \frac{0.05}{60}$ in each tissue. Variants were grouped into four categories: three categories (direct, vertical, confounder) for PRISM significant variant effects, and a category for GWAS significant associations. For each tissue, we then determined the number of unique eGenes significantly paired with variants separately in each one of the four categories. Finally, for each tissue, we calculated the enrichment in unique genes of each category as: $\frac{\text{Number of eGenes in category within tissue}}{\text{Number of eGenes in category across all tissues}} / \frac{\text{Number of eGenes within tissue across all categories}}{\text{Total number of eGenes across all tissues and categories}}$

Gene networks and pathways analysis

We configured FUMA with specific parameters to ensure accurate and reliable results. We used Ensembl version 110 as the reference, and the UK Biobank release 2b population dataset “WBrits10k” was chosen as the reference panel. A physical mapping window of 10 kb was employed to precisely map variants to nearby genes. We set the significance threshold p-value $< 5 \times 10^{-8}$ for GWAS and p-value $< \frac{5\times10^{-8}}{60}$ for PRISM direct variants. Additionally, we incorporated eQTL mapping into our analysis using GTEx

data version 6, including all available tissue types. Next, using FUMA results, we conducted pathway enrichment analyses with Metascape[45] on DisGeNET[39] pathways for genes mapped to GWAS and PRISM direct variants. These analyses were performed separately for 48 traits with identified gene sets. We performed a paired Student test to assess the significance of differences in pathway enrichments between PRISM and GWAS, with significance threshold p-value $< 1 \times 10^{-3}$. Finally, we constructed bipartite networks, which consist of two distinct sets of nodes (here, genes and traits) where edges only exist between nodes of different sets. Edges were added between traits and their associated genes. The degree centrality of a trait, indicating the number of associated genes, was calculated as: $\frac{\text{Number of edges incident to trait}}{\text{Total number of traits in the network}}$. Betweenness centrality, measuring the extent to which a trait lies on the shortest paths between other traits, was calculated as: $\frac{\text{Number of shortest paths passing through the trait}}{\text{Total number of shortest paths}}$. Closeness centrality, assessing the proximity of a trait to all other traits in the network, was calculated as $\frac{1}{\text{Sum of shortest distances from the trait to all other traits}}$.

Availability of the method and results.

PRISM is implemented in R and a user-friendly tutorial is available on github. As long as GWAS summary statistics are available and the studied variants are mapped in HapMap3, PRISM can compute any network of traits of interest to distinguish direct variant-trait effects from vertical and confounder variant-trait effects. To fulfill the assumptions of the paired Student test used by PRISM, we recommend to include at least 31 traits. PRISM results are available on Zenodo or easily accessible through an online user-friendly interface. Indeed, we developed a ShinyR interface, freely available online, to display PRISM results on our network of 61 highly heritable traits. Results can be visualized at the trait level and also to display the causal network of any genetic variant of interest.

Funding

MT, AN, and MV are supported by the French National Research Agency (ANR) (ANR-21-CE45-0023-01). MT and MFM are supported by the data intelligence institute of Paris (diiP, IdEx Université Paris Cité, ANR-18-IDEX-0001). MT is a PhD student from the FIRE PhD program funded by the Bettencourt Schueller foundation and the EURIP graduate program (ANR-17-EURE-0012).

Authors contributions

MT contributed to study conception, data analysis, interpretation of the results, drafting and critical revisions of the manuscript; AN contributed to data analysis, interpretation of the results and revision of the manuscript; MFM contributed to revision of the manuscript; YR contributed to study conception and revision of the manuscript; MV supervised the study and contributed to study conception, data analysis, interpretation of the results and critical revision of the manuscript.

References

1. Loos, R. J. F. 15 years of genome-wide association studies and no signs of slowing down. *Nature Communications* **11**, 5900 (2020).

2. Uffelmann, E. *et al.* Genome-wide association studies. *Nature Reviews Methods Primers* **1**, 1–21 (2021).

3. MacArthur, J. *et al.* The new NHGRI-EBI Catalog of published genome-wide association studies (GWAS Catalog). *Nucleic Acids Research* **45**, D896–D901 (2017).

4. Chesmore, K., Bartlett, J. & Williams, S. M. The ubiquity of pleiotropy in human disease. *Human Genetics* **137**, 39–44 (2018).

5. Solovieff, N., Cotsapas, C., Lee, P. H., Purcell, S. M. & Smoller, J. W. Pleiotropy in complex traits: Challenges and strategies. *Nature Reviews. Genetics* **14**, 483–495 (2013).

6. Gratten, J. & Visscher, P. M. Genetic pleiotropy in complex traits and diseases: Implications for genomic medicine. *Genome Medicine* **8**, 78 (2016).

7. Jordan, D. M., Verbanck, M. & Do, R. HOPS: A quantitative score reveals pervasive horizontal pleiotropy in human genetic variation is driven by extreme polygenicity of human traits and diseases. *Genome Biology* **20**, 222 (2019).

8. Nicolae, D. L. *et al.* Trait-Associated SNPs Are More Likely to Be eQTLs: Annotation to Enhance Discovery from GWAS. *PLoS Genetics* **6**, e1000888 (2010).

9. Alsheikh, A. J. *et al.* The landscape of GWAS validation; systematic review identifying 309 validated non-coding variants across 130 human diseases. *BMC Medical Genomics* **15**, 74 (2022).

10. Hormozdiari, F., Kostem, E., Kang, E. Y., Pasaniuc, B. & Eskin, E. Identifying Causal Variants at Loci with Multiple Signals of Association. *Genetics* **198**, 497–508 (2014).

11. Schaid, D. J., Chen, W. & Larson, N. B. From genome-wide associations to candidate causal variants by statistical fine-mapping. *Nature Reviews Genetics* **19**, 491–504 (2018).

12. Fisher, V., Sebastiani, P., Cupples, L. A. & Liu, C.-T. ANNORE: Genetic fine-mapping with functional annotation. *Human Molecular Genetics* **31**, 32–40 (2022).

13. Yang, Z. *et al.* CARMA is a new Bayesian model for fine-mapping in genome-wide association meta-analyses. *Nature Genetics* **55**, 1057–1065 (2023).

14. Kichaev, G. *et al.* Integrating Functional Data to Prioritize Causal Variants in Statistical Fine-Mapping Studies. *PLOS Genetics* **10**, e1004722 (2014).

15. Umans, B. D., Battle, A. & Gilad, Y. Where Are the Disease-Associated eQTLs? *Trends in Genetics* **37**, 109–124 (2021).

16. Connally, N. J. *et al.* The missing link between genetic association and regulatory function. *eLife* **11**, e74970 (2022).

17. Mostafavi, H., Spence, J. P., Naqvi, S. & Pritchard, J. K. Systematic differences in discovery of genetic effects on gene expression and complex traits. *Nature Genetics* **55**, 1866–1875 (2023).

18. Battram, T., Gaunt, T. R., Relton, C. L., Timpson, N. J. & Hemani, G. A comparison of the genes and genesets identified by GWAS and EWAS of fifteen complex traits. *Nature Communications* **13**, 7816 (2022).

19. Verbanck, M., Chen, C.-Y., Neale, B. & Do, R. Detection of widespread horizontal pleiotropy in causal relationships inferred from Mendelian randomization between complex traits and diseases. *Nature Genetics* 1 (2018) doi:10.1038/s41588-018-0099-7.

20. Darrous, L., Mounier, N. & Kutalik, Z. Simultaneous estimation of bi-directional causal effects and heritable confounding from GWAS summary statistics. *Nature Communications* **12**, 7274 (2021).

21. Morrison, J., Knoblauch, N., Marcus, J. H., Stephens, M. & He, X. Mendelian randomization accounting for correlated and uncorrelated pleiotropic effects using genome-wide summary statistics. *Nature Genetics* 1–8 (2020) doi:10.1038/s41588-020-0631-4.

22. Cheng, Q., Zhang, X., Chen, L. S. & Liu, J. Mendelian randomization accounting for complex correlated horizontal pleiotropy while elucidating shared genetic etiology. *Nature Communications* **13**, 6490 (2022).

23. Bycroft, C. *et al.* The UK Biobank resource with deep phenotyping and genomic data. *Nature* **562**, 203–209 (2018).

24. Wang, G., Sarkar, A., Carbonetto, P. & Stephens, M. A Simple New Approach to Variable Selection in Regression, with Application to Genetic Fine Mapping. *Journal of the Royal Statistical Society Series B: Statistical Methodology* **82**, 1273–1300 (2020).

25. Zou, Y., Carbonetto, P., Wang, G. & Stephens, M. Fine-mapping from summary data with the 'Sum of Single Effects' model. *PLOS Genetics* **18**, e1010299 (19 juil. 2022).

26. Benner, C. *et al.* FINEMAP: Efficient variable selection using summary data from genome-wide association studies. *Bioinformatics* **32**, 1493–1501 (2016).

27. Xie, F., Wang, D. & Cheng, M. CDKN2B-AS1 may act as miR-92a-3p sponge in coronary artery disease. *Minerva Cardiology and Angiology* **72**, (2024).

28. Rogg, E.-M. *et al.* Analysis of Cell Type-Specific Effects of MicroRNA-92a Provides Novel Insights Into Target Regulation and Mechanism of Action. *Circulation* **138**, 2545–2558 (2018).

29. Carena, M. C. *et al.* Role of Human Epicardial Adipose Tissue–Derived miR-92a-3p in Myocardial Redox State. *Journal of the American College of Cardiology* **82**, 317–332 (2023).

30. Wang, W. *et al.* Circulating microRNA-92a level predicts acute coronary syndrome in diabetic patients with coronary heart disease. *Lipids in Health and Disease* **18**, 22 (2019).

31. ReproGen Consortium *et al.* Partitioning heritability by functional annotation using genome-wide association summary statistics. *Nature Genetics* **47**, 1228–1235 (2015).

32. Hartmann, K., Seweryn, M. & Sadee, W. Interpreting coronary artery disease GWAS results: A functional genomics approach assessing biological significance. *PLOS ONE* **17**, e0244904 (2022).

33. Conlon, D. M. *et al.* Sortilin restricts secretion of apolipoprotein B-100 by hepatocytes under stressed but not basal conditions. *The Journal of Clinical Investigation* **132**, (2022).

34. Sniderman, A. D. *et al.* Apolipoprotein B Particles and Cardiovascular Disease: A Narrative Review. *JAMA Cardiology* **4**, 1287–1295 (2019).

35. Asghari, G. *et al.* Association of Rs2282679 polymorphism in vitamin D binding protein gene (GC) with the risk of vitamin D deficiency in an iranian population: Season-specific vitamin D status. *BMC Endocrine Disorders* **23**, 217 (2023).

36. Kew, R. R. The Vitamin D Binding Protein and Inflammatory Injury: A Mediator or Sentinel of Tissue Damage? *Frontiers in Endocrinology* **10**, 470 (2019).

37. The GTEx Consortium *et al.* The GTEx Consortium atlas of genetic regulatory effects across human tissues. *Science* **369**, 1318–1330 (2020).

38. Watanabe, K., Taskesen, E., Van Bochoven, A. & Posthuma, D. Functional mapping and annotation of genetic associations with FUMA. *Nature Communications* **8**, 1826 (2017).

39. Piñero, J. *et al.* DisGeNET: A comprehensive platform integrating information on human disease-associated genes and variants. *Nucleic Acids Research* **45**, D833–D839 (2017).

40. Bulik-Sullivan, B. K. *et al.* LD Score regression distinguishes confounding from polygenicity in genome-wide association studies. *Nature Genetics* **47**, 291 (2015).

41. Mounier, N. & Kutalik, Z. Bias correction for inverse variance weighting Mendelian randomization. *Genetic Epidemiology* **47**, 314–331 (2023).

42. Chen, W., Coombes, B. J. & Larson, N. B. Recent advances and challenges of rare variant association analysis in the biobank sequencing era. *Frontiers in Genetics* **13**, 1014947 (2022).

43. Hou, L. *et al.* MRSL: A causal network pruning algorithm based on GWAS summary data. *Briefings in Bioinformatics* **25**, bbae086 (2024).

44. Devuyst, O. The 1000 Genomes Project: Welcome to a New World. *Peritoneal Dialysis International: Journal of the International Society for Peritoneal Dialysis* **35**, 676–677 (2015).

45. Zhou, Y. *et al.* Metascape provides a biologist-oriented resource for the analysis of systems-level datasets. *Nature Communications* **10**, 1523 (2019).

A) Hypothesis of PRISM

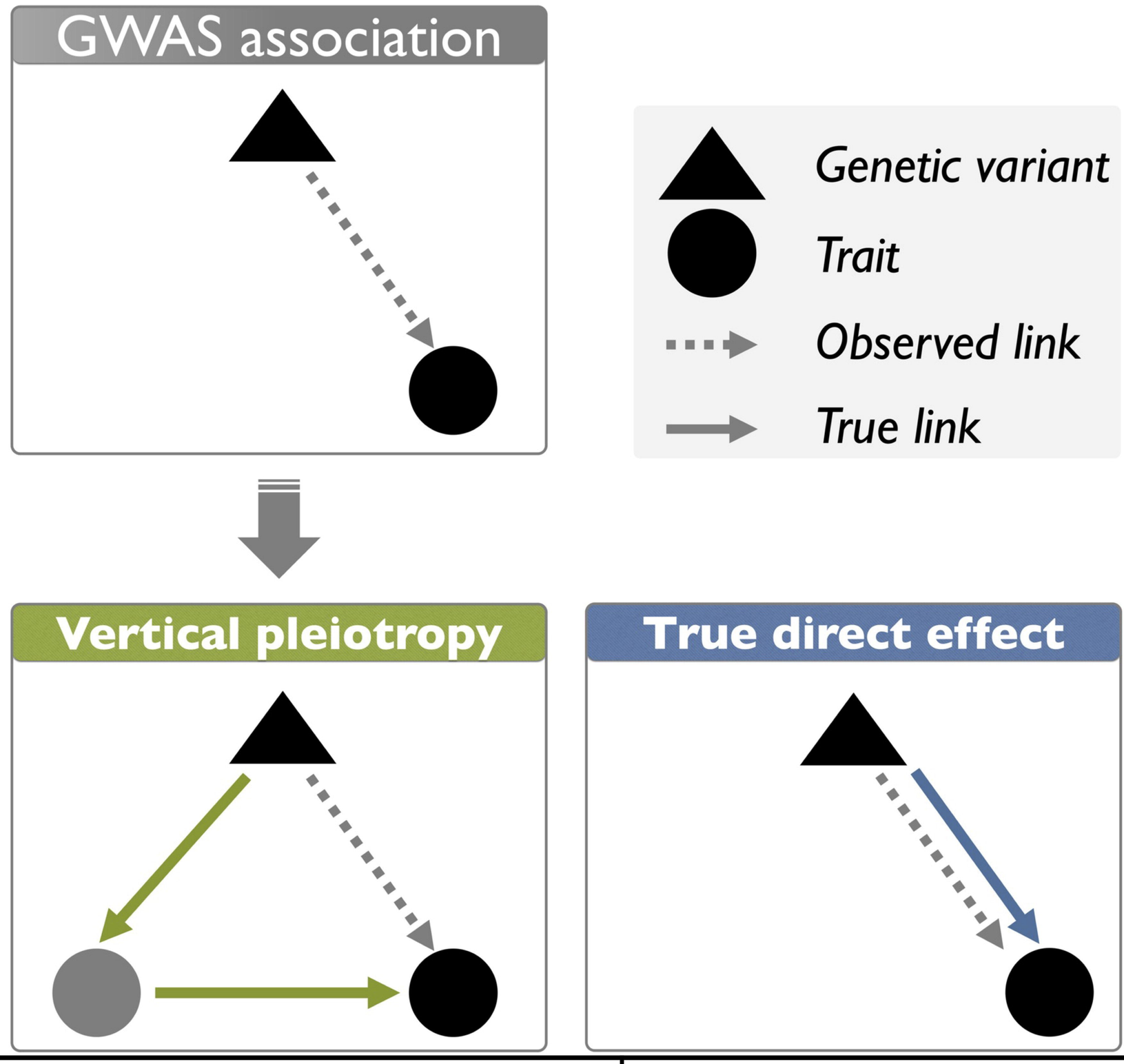

B) Aim of PRISM

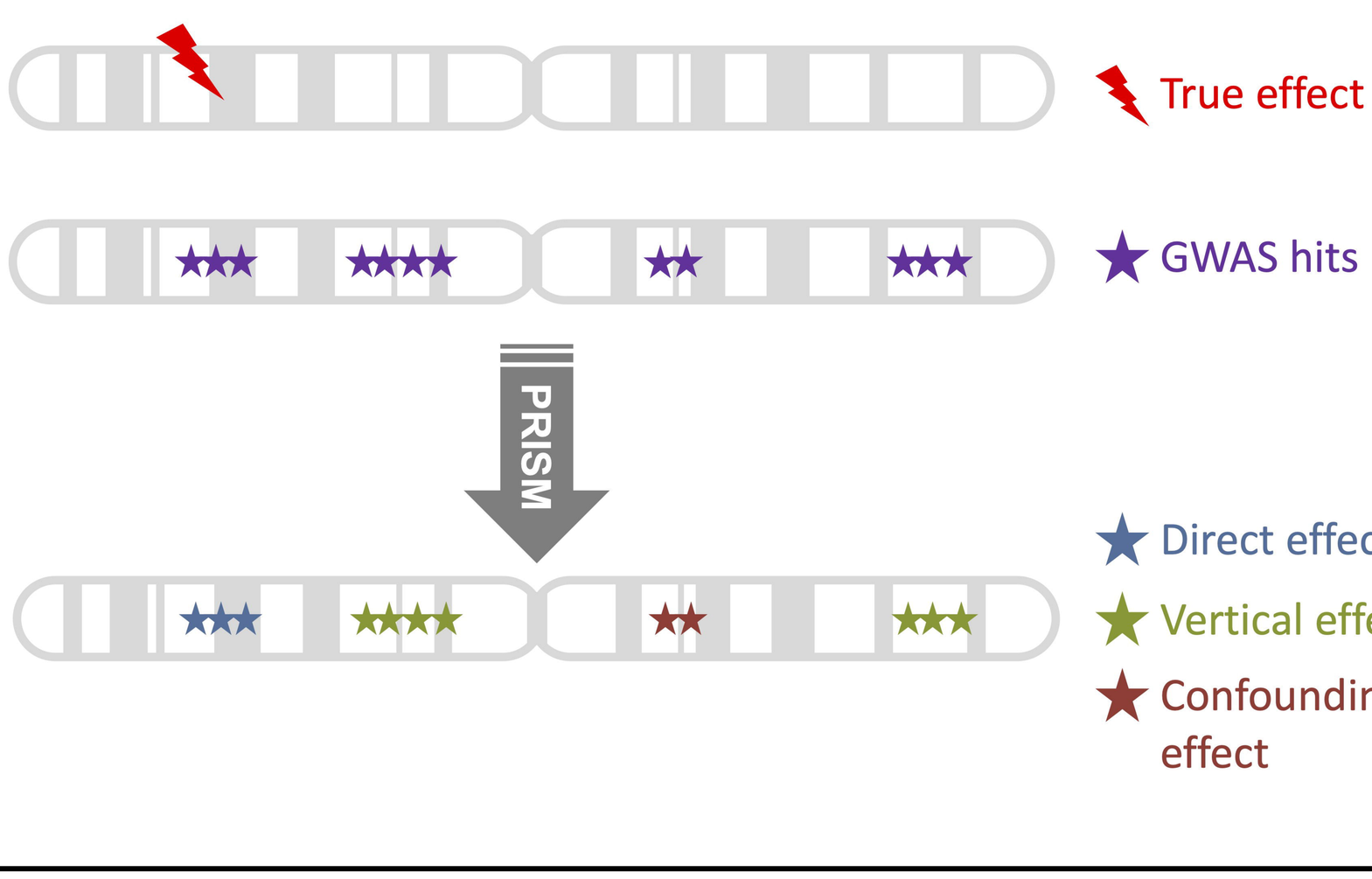

C) Trait relationships

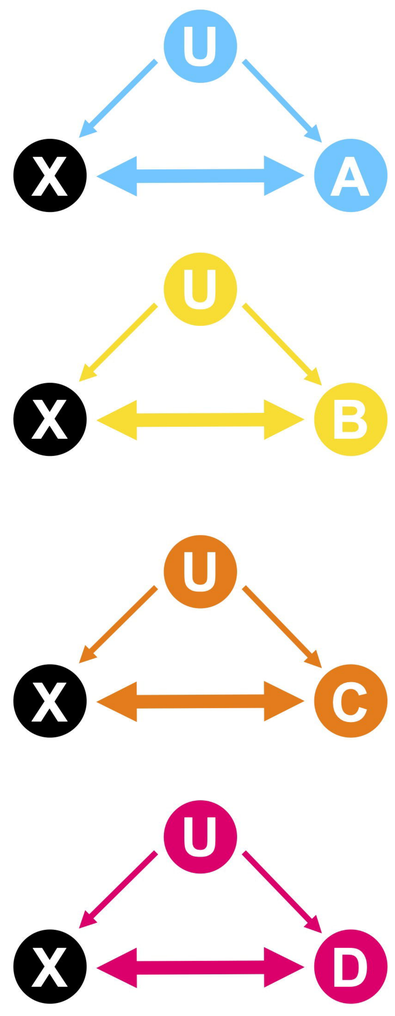

D) Principle of PRISM

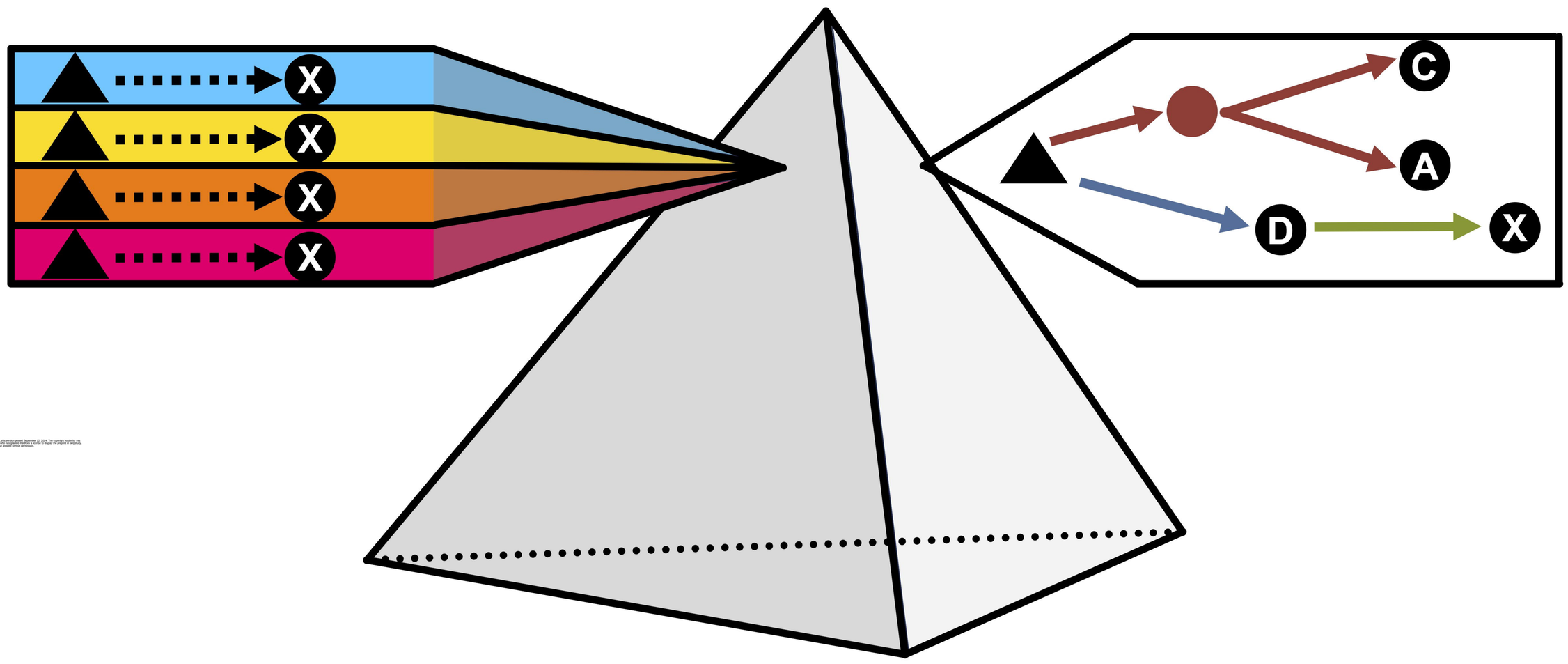

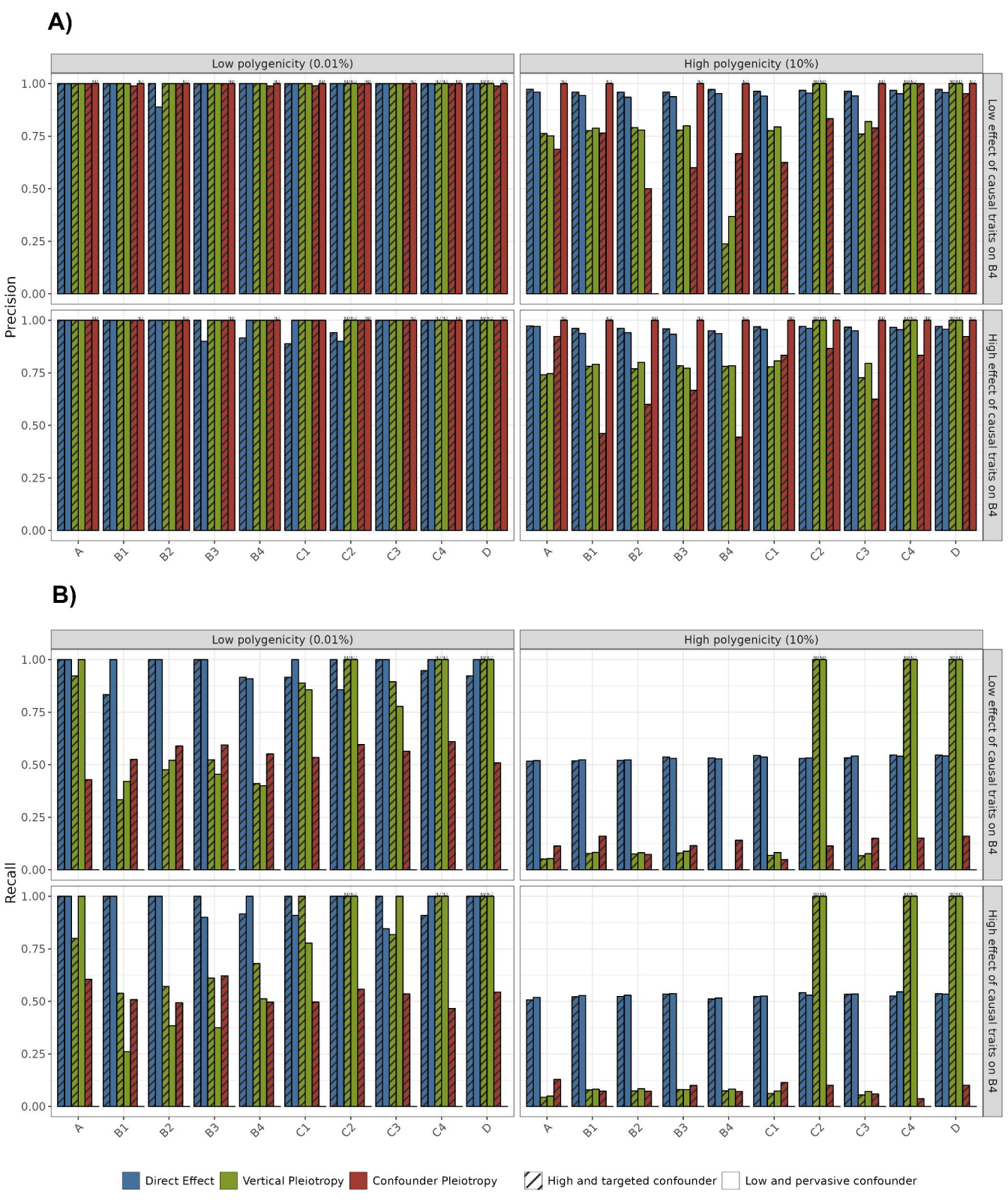
A)
Low polygenicity (0.01%)
High polygenicity (10%)
Low effect of causal traits on B4
High effect of causal traits on B4
Precision
1.00
0.75
0.50
0.25
0.00
A
B1
B2
B3
B4
C1
C2
C3
C4
D
B)
Recall
Direct Effect
Vertical Pleiotropy
Confounder Pleiotropy
High and targeted confounder
Low and pervasive confounder


Forced vital capacity
Asthma
Mental disorders
Neuroticism score
CHD
DBP
Basal metabolic rate
Gout
T2D
Hypertension
Triglycerides
LDL-C
HDL-C
Cholesterol
Apoliprotein B
Apoliprotein A
Never smoker
Muesli intake
Alcohol freq
Cereal intake
Insomnia
Physical activity
UC
Overall health rating
University degree
Match identification exercise
Cancer
Breast cancer
Skin cancer
Pancreas cancer
Reticulocyte count
Lymphocyte percentage
Neutrophil count
Monocyte count
Lymphocyte count
Platelet count
Red blood cell count
White blood cell count
Basophil count
Eosinophil count
Vitamin D
Urate
Total protein
Testosterone
Phosphate
IGF-1
HbA1C
Glucose
Gamma glutamyltransferase
CRP
Creatinine
Calcium
Aspartate aminotransferase
Alanine aminotransferase
Albumin
Standing height
Waist circumference
BMD
Body impedance
Body fat percentage
BMI
BMI
Body fat percentage
Body impedance
BMD
Waist circumference
Standing height
Albumin
Alanine aminotransferase
Aspartate aminotransferase
Calcium
Creatinine
CRP
Gamma glutamyltransferase
Glucose
HbA1C
IGF-1
Phosphate
Testosterone
Total protein
Urate
Vitamin D
Eosinophil count
Basophil count
White blood cell count
Red blood cell count
Platelet count
Lymphocyte count
Monocyte count
Neutrophil count
Lymphocyte percentage
Reticulocyte count
Pancreas cancer
Skin cancer
Breast cancer
Cancer
Match identification exercise
University degree
Overall health rating
UC
Physical activity
Insomnia
Cereal intake
Alcohol freq
Muesli intake
Never smoker
Apoliprotein A
Apoliprotein B
Cholesterol
HDL-C
LDL-C
Triglycerides
Hypertension
T2D
Gout
Basal metabolic rate
DBP
CHD
Neuroticism score
Mental disorders
Asthma
Forced vital capacity

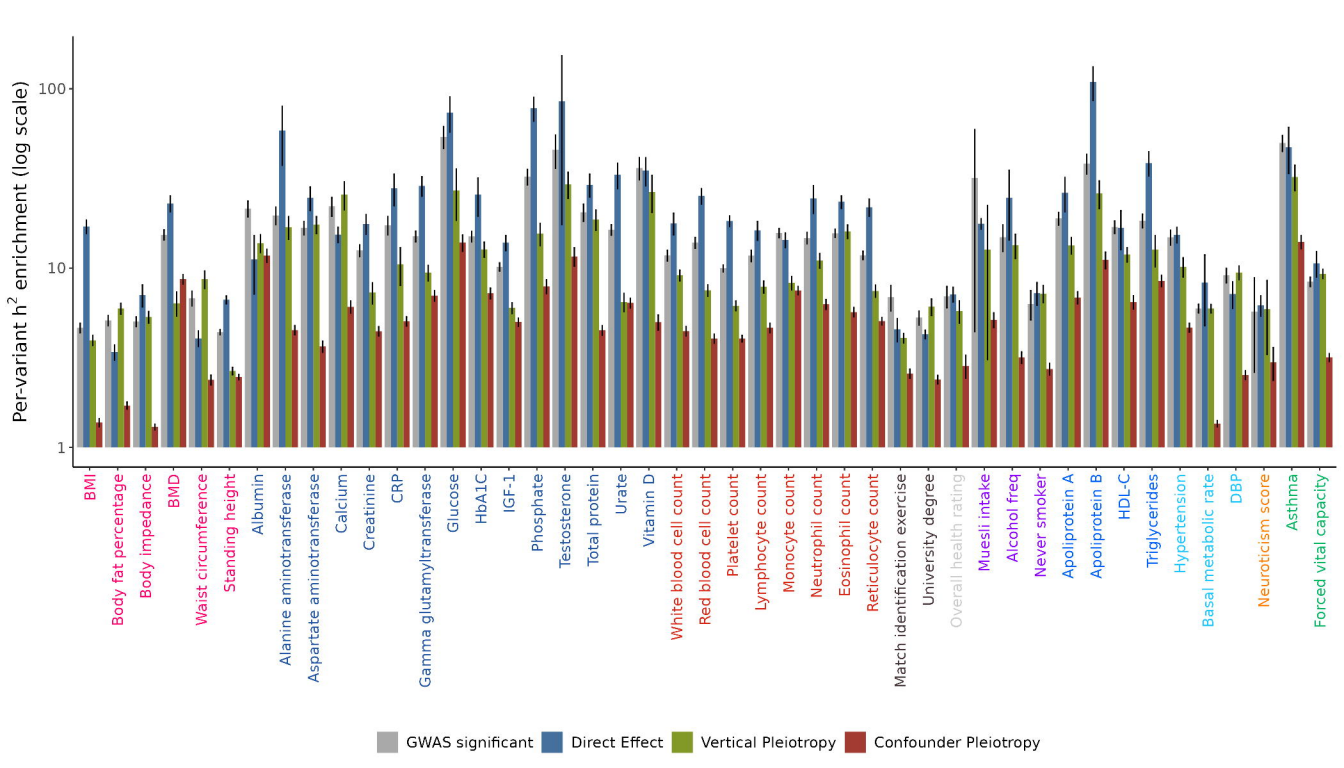
Per-variant h2 enrichment (log scale)
100
10
1
BMI
Body fat percentage
Body impedance
BMD
Waist circumference
Standing height
Albumin
Alanine aminotransferase
Aspartate aminotransferase
Calcium
Creatinine
CRP
Gamma glutamyltransferase
Glucose
HbA1C
IGF-1
Phosphate
Testosterone
Total protein
Urate
Vitamin D
White blood cell count
Red blood cell count
Platelet count
Lymphocyte count
Monocyte count
Neutrophil count
Eosinophil count
Reticulocyte count
Match identification exercise
University degree
Overall health rating
Muesli intake
Alcohol freq
Never smoker
Apoliprotein A
Apoliprotein B
HDL-C
Triglycerides
Hypertension
Basal metabolic rate
DBP
Neuroticism score
Asthma
Forced vital capacity
GWAS significant
Direct Effect
Vertical Pleiotropy
Confounder Pleiotropy